Journal of Sound and Vibration (2001) **244**(5), 837–858
doi:10.1006/jsvi.2000.3532, available online at http://www.idealibrary.com on IDEAL®

TWO-DIMENSIONAL TRANSIENT WAVE PROPAGATION IN VISCOELASTIC LAYERED MEDIA

I. Abu Alshaikh, D. Turhan and Y. Mengi

Department of Engineering Sciences, Middle East Technical University, Ankara 06531, *Turkey*.
E-mail: *turhan@metu.edu.tr*

(*Received* 8 *August* 2000, *and in final form* 6 *December* 2000)

Propagation of two-dimensional transient waves in multilayered viscoelastic media is investigated. The multilayered medium consists of N different isotropic, homogeneous and linearly viscoelastic layers with more than one discrete relaxation time. The top surface of the layered medium is subjected to dynamic in-plane surface tractions; whereas, the lower surface is free or fixed. A numerical technique which combines the Fourier transform with the method of characteristics is employed to obtain the solutions. The numerical results are displayed in curves denoting the variations of the stress and displacement components with time at different locations. These curves reveal clearly the scattering effects caused by the reflections and refractions of waves at the boundaries and at the interfaces of the layers. The curves also display the effects of viscous damping in the wave profiles. By suitably adjusting the material constants, curves for the cases of elastic layers and viscoelastic layers with one relaxation time (standard linear solid) are also obtained. The curves further show that the numerical technique applied in this study is capable of predicting the sharp variations in the field variables in the neighborhood of the wave fronts. Solutions for some special cases, including Lamb's problem for the elastic half-space, are obtained and compared with the existing solutions in the literature; very good agreement is found.

1. INTRODUCTION

The study of elastic wave propagation in layered media has been a subject of extensive investigation in the literature. It is of considerable importance in a variety of applications ranging from seismology to laminated composites used in aircraft, spacecraft and other engineering structures, and to non-destructive evaluation of laminated composites.

Early analytical treatment of the subject can be found in the books by Ewing *et al.* [1] and Brekhovskikh [2]. Approximate models have been developed to study the propagation of harmonic and transient waves which yield satisfactory results when the thicknesses of the layers are small compared to the wavelengths of the propagating waves [3–7]. Harmonic wave propagation in layered elastic media with isotropic and anisotropic layers has also been investigated by more exact methods of elasticity theory which are valid for any wavelength [8–12]. Transient axisymmetric wave propagation in weakly coupled layered structures is investigated in references [13, 14]. Two different computational approaches, one based on the numerical inversion of Fourier and Hankel transforms and the other the finite element method, are employed in reference [14]. Rizzi and Doyle [15] developed a spectral element approach based on fast Fourier transform and applied it to study transient waves in elastic layered solids. The transfer matrix method was employed by Kundu and Mal [16] to study wave propagation in multilayered solids with isotropic layers

0022-460X/01/300837 + 22 $35.00/0

and by Mal [17] in laminated composites with anisotropic layers, namely transversely isotropic layers, subjected to periodic surface loads. A multiple transform technique coupled with a matrix method was used to investigate the elastodynamic response of a uni-directional composite laminate to concentrated surface loads in references [18, 19] and multilayered composite laminates consisting of transversely isotropic layers with arbitrarily oriented symmetry axes to dynamic surface loads in reference [20]. The transversely isotropic layers are assumed to be dissipative and the dissipative property is modelled approximately through the introduction of a frequency-dependent damping function in reference [20]. A generalized Thomson–Haskell matrix method was proposed by Jianfeng and Youming [21] for modelling elastic wave propagation in stratified media with laterally homogeneous and laterally inhomogeneous layers. Transient waves excited by impact loads in anisotropic laminated plates were investigated by Liu *et al.* [22, 23] by employing a numerical method which combines the finite element method and the Fourier transform technique. Modal analysis is introduced in the finite element method and fast Fourier transform algorithm is used in the inversion of the Fourier transforms in references [22, 23]. Harmonic and transient wave propagation in elastic layered media with isotropic and anisotropic layers are also investigated in the books by Tygel and Hubral [24], Achenbach [25], Miklowitz [26], Nayfeh [27] and Van der Hijden [28]. Elegant analytical and numerical techniques based on the Green function formulations, integral transforms, inversion of integral transforms by Cagniard-de Hoop method and asymptotic techniques can be found in these books [24–28].

Compared to the extensive literature on elastic wave propagation in multilayered elastic media, relatively less work can be found on transient wave propagation in viscoelastic layered media. Most of the existing literature on transient waves in viscoelastic laminates has focused on one-dimensional wave propagation normal to the layering of the laminate [29–32]. A two-dimensional problem concerning the propagation of coupled P and S waves parallel to the layers in a semi-infinite plate consisting of a linearly viscoelastic layer sandwiched between two identical linearly elastic layers was investigated by Nkemzi and Green [33]. Xu and Mal [34] calculated the in-plane Green function for a layered viscoelastic solid.

In this study, propagation of two-dimensional transient waves in viscoelastic layered media consisting of N different layers is investigated. The layers of the multilayered medium are isotropic, homogeneous and linearly viscoelastic with discrete relaxation spectra involving two time constants. By suitably adjusting the material constants, the case of multilayered elastic media is treated as a special case as well.

A numerical technique which combines the Fourier transform with the method of characteristics is employed to obtain the solution. The method of characteristics has been employed effectively in investigating one-dimensional transient wave propagation problems in layered media. Among many contributions in this area, we can mention those of Chou and Greif [35] in layered elastic media, of Turhan and Calayír [36] in viscoelastic layered media with layers modelled as standard linear solid, and of Turhan *et al.* [37] in thermoelastic layered media. In multi-dimensional wave propagation problems, however, the construction of the solution by the method of characteristics becomes difficult and impractical. In this study, the shortcomings of the method of characteristics for multi-dimensional wave propagation analysis are eliminated by employing a numerical technique which combines the Fourier transform technique with the one-dimensional method of characteristics. Such a numerical technique was first introduced by Mengi and Tanríkulu [38] and later applied by Tanríkulu *et al.* [39] to assess an approximate theory developed for plates and layered composites [40]. Because of the inclusion of the method of characteristics in the analysis, the numerical technique employed is capable of describing

the sharp variations of the disturbances in the neighborhood of the wave fronts. Hence, it can be used conveniently in multi-dimensional transient wave propagation analyses.

2. FORMULATION OF THE PROBLEM

The multilayered medium considered in this study is of thickness H and consists of N different layers; see Figure 1. It is referred to a Cartesian co-ordinate system, x_i, in which the x_1x_3- plane coincides with the top surface of the layered medium and the x_2-axis is directed downwards. The top surface of the layered medium is subjected to dynamic in-plane surface tractions; whereas, the lower surface is free, fixed or subjected to in-plane surface tractions as well. The surface tractions can be normal stresses or in-plane shear stresses. In the formulation, it is assumed that the surface tractions are arbitrary functions of x_1 and time t; but they are uniform and extend to infinity in the x_3 direction. The layers of the composite medium are assumed to be perfectly bonded to each other. Furthermore, the layered medium is assumed to be initially at rest.

The problem is a two-dimensional plane strain problem; hence, the displacement component u_3 vanishes identically and the displacement components u_1 and u_2 are functions of x_1, x_2 and t: i.e., $u_1 = u_1(x_1, x_2, t)$ and $u_2 = u_2(x_1, x_2, t)$. Thus, the stress equations of motion for a typical layer can be written as

$$\frac{\partial \tau_{11}}{\partial x_1} + \frac{\partial \tau_{12}}{\partial x_2} = \rho \frac{\partial v_1}{\partial t}, \qquad \frac{\partial \tau_{12}}{\partial x_1} + \frac{\partial \tau_{22}}{\partial x_2} = \rho \frac{\partial v_2}{\partial t}, \tag{2.1}$$

where $\tau_{11}, \tau_{12}, \tau_{22}$ are the stress components, $v_1 = \partial u_1/\partial t$ and $v_2 = \partial u_2/\partial t$ are the components of the particle velocity in the x_1 and x_2 directions, respectively, and ρ is the mass density of the typical layer considered.

The layers of the multilayered medium are assumed to be isotropic and linearly viscoelastic for which the constitutive equations can be written as [41]

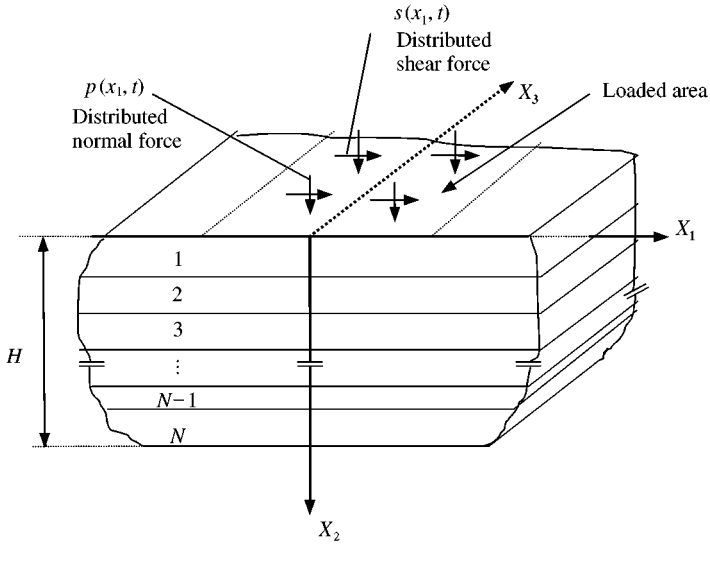

Figure 1. Layered medium subjected to in-plane surface tractions.

$$P_1(D)\tau'_{ij} = Q_1(D)\varepsilon'_{ij}, \qquad P_2(D)\tau_{kk} = Q_2(D)\,\varepsilon_{kk}, \tag{2.2}$$

where

$$P_1(D) = \sum_{m=0}^{n} a_m D^m, \qquad Q_1(D) = \sum_{m=0}^{n} b_m D^m,$$

$$P_2(D) = \sum_{m=0}^{n} c_m D^m, \qquad Q_2(D) = \sum_{m=0}^{n} d_m D^m, \tag{2.3}$$

in which a_m, b_m, c_m, d_m are specified constants for a typical layer and $D^m = \partial^m/\partial t^m$. In the above equations and in the developments that will follow, when it is appropriate, the indicial notation and all of the rules that apply to its use are employed. In equations (2.2), $\tau'_{ij}, \varepsilon'_{ij}$ are the components of the stress and strain deviators defined by

$$\tau'_{ij} = \tau_{ij} - \tfrac{1}{3}\delta_{ij}\tau_{kk}, \qquad \varepsilon'_{ij} = \varepsilon_{ij} - \tfrac{1}{3}\delta_{ij}\varepsilon_{kk}, \tag{2.4}$$

where δ_{ij} is the Kronecker delta. If the initial values of $\tau'_{ij}, \varepsilon'_{ij}, \tau_{kk}, \varepsilon_{kk}$ satisfy certain conditions [41] the constitutive equations, equations (2.2), can be written in terms of integral equations as

$$\tau'_{ij}(x,t) = G_1(t)\varepsilon'_{ij}(x,0) + \int_0^t G_1(t-\tau)\frac{\partial \varepsilon'_{ij}}{\partial \tau}(x,\tau)\,\mathrm{d}\tau$$

$$\tau_{kk}(x,t) = G_2(t)\varepsilon_{kk}(x,0) + \int_0^t G_2(t-\tau)\frac{\partial \varepsilon_{kk}}{\partial \tau}(x,\tau)\,\mathrm{d}\tau, \tag{2.5}$$

where $G_1(t), G_2(t)$ are the shear and bulk relaxation functions, respectively, and x is the position vector of the particle considered. The relaxation functions in equations (2.5) can be expressed in the forms

$$G_1(t) = 2\mu\left[\alpha_0 + \sum_{m=1}^{n} \alpha_m \mathrm{e}^{-t/\tau_m}\right], \qquad G_2(t) = (2\mu + 3\lambda)\left[\beta_0 + \sum_{m=1}^{n} \beta_m\,\mathrm{e}^{-\tau/\zeta_m}\right], \tag{2.6}$$

where $\mu = G_1(0)/2$, $(\frac{2}{3}\mu + \lambda) = G_2(0)/3$, τ_m, ζ_m are some positive constants and α_m, β_m are positive non-dimensional constants such that

$$\sum_{m=0}^{n} \alpha_m = 1, \qquad \sum_{m=0}^{n} \beta_m = 1. \tag{2.7}$$

Here, it may be noted that equations (2.6) represent the generalized Maxwell model [42]; where τ_m and ζ_m are retardation (relaxation) times, and α_m and β_m are the corresponding relaxation coefficients for the shear and bulk moduli, respectively. The inclusion of more terms in equations (2.6) would facilitate fitting the relaxation functions given in these equations to experimental data. It may also be observed that, in view of the conditions given in equations (2.7), μ and $(\frac{2}{3}\mu + \lambda)$ in equations (2.6) represent the instantaneous values of the shear and bulk relaxation functions respectively.

In this study, the viscoelastic solid is modelled with n = 2 in equations (2.3) and (2.6). Constitutive equations of the same form were used by Wegner and Haddow [43], Jiang and Haddow [32] and Wegner [44] in various one-dimensional transient wave propagation problems in viscoelastic media. Equations (2.3) and (2.6) with $n = 1$ represent the constitutive equations for a standard linear solid.

There are two reasons for choosing $n = 2$ here. First, taking $n > 2$ complicates the numerical analysis considerably, which is, as mentioned in "Introduction", carried out by using a special method combining the method of characteristics with Fourier transform technique. Secondly, one can think that the constitutive equations (equations (2.2), (2.3) and (2.6)) with $n = 2$ would be adequate to represent the response of viscoelastic materials, in particular, of thermoset and thermoplastic polymers, in the region around the glass-transition temperature.

The constants in equations (2.3) and (2.6) with $n = 2$ are related according to [43]

$$a_0 = (\tau_1\tau_2)^{-1}, \qquad a_1 = (\tau_1 + \tau_2)/\tau_1\tau_2, \qquad a_2 = 1, \qquad b_0 = 2\mu\alpha_0/\tau_1\tau_2,$$

$$b_1 = 2\mu[\tau_1(\alpha_0 + \alpha_1) + \tau_2(\alpha_0 + \alpha_2)]/\tau_1\tau_2, \qquad b_2 = 2\mu,$$

$$c_0 = (\zeta_1\zeta_2)^{-1}, \qquad c_1 = (\zeta_1 + \zeta_2)/\zeta_1\zeta_2, \qquad c_2 = 1, \qquad d_0 = (2\mu + 3\lambda)\,\beta_0/\zeta_1\zeta_2,$$

$$d_1 = (2\mu + 3\lambda)[\zeta_1(\beta_0 + \beta_1) + \zeta_2(\beta_0 + \beta_2)]/\zeta_1\zeta_2, \qquad d_2 = (2\mu + 3\lambda). \tag{2.8}$$

The non-zero strain components for the plane strain problem considered here are related to the displacement components u_1 and u_2 through

$$\varepsilon_{11} = \frac{\partial u_1}{\partial x_1}, \qquad \varepsilon_{22} = \frac{\partial u_2}{\partial x_2}, \qquad \varepsilon_{12} = \tfrac{1}{2}\left(\frac{\partial u_1}{\partial x_2} + \frac{\partial u_2}{\partial x_1}\right). \tag{2.9}$$

The formulation of the problem is completed by stating the boundary, initial and interface conditions. The boundary conditions at the top surface $x_2 = 0$ of the multilayered medium are

$$\tau_{22}(x_1, 0, t) = -\,p(x_1, t), \qquad \tau_{12}(x_1, 0, t) = 0, \tag{2.10}$$

or

$$\tau_{12}(x_1, 0, t) = -\,s(x_1, t), \qquad \tau_{22}(x_1, 0, t) = 0, \tag{2.11}$$

where $p(x_1, t)$ and $s(x_1, t)$ are prescribed functions of x_1 and t. The bottom surface $x_2 = H$ is either free of surface tractions or fixed. Hence, the boundary conditions can be written as

$$\tau_{22}(x_1, H, t) = 0, \qquad \tau_{12}(x_1, H, t) = 0, \tag{2.12}$$

or

$$u_1(x_1, H, t) = 0, \qquad u_2\,(x_1, H, t) = 0. \tag{2.13}$$

In the method employed in this paper, note that other alternatives for boundary conditions, such as in-plane surface tractions on the bottom surface, or mixed–mixed boundary conditions, i.e., one component of displacement and the other component of the in-plane surface tractions, can be handled with equal ease on both surfaces. The multilayered medium is assumed to be initially at rest; hence, all the field variables are zero at $t = 0$. The layers of the multilayered medium are assumed to be perfectly bonded to each other. Hence, the interface conditions imply that τ_{22}, τ_{12} and u_1, u_2 are continuous across the interfaces of the layers. The formulation of the problem is thus complete.

The governing field equations, equations (2.1), (2.2) and (2.9), will now be applied to each layer and the solutions will be required to satisfy the continuity conditions at the interfaces,

the boundary conditions at the top and bottom surfaces, equations (2.10)-(2.13), and quiescent initial conditions.

3. SOLUTION OF THE PROBLEM

The solution is obtained by employing a numerical technique which combines the Fourier transform with the method of characteristics. The technique involves first the application of the Fourier transform to the governing equations over the space variable x_1, then the integration of the resulting one-dimensional hyperbolic equations by the method of characteristics, and finally inverting the solution back into real space. For this purpose, one can first write the constitutive equations for the typical layer considered, equations (2.2), in view of equations (2.3) and (2.4) with $n = 2$ and $a_2 = c_2 = 1$, as

$$\frac{\partial T_{11}}{\partial t} - \frac{1}{3}\frac{\partial T_{kk}}{\partial t} + a_0\tau_{11} + a_1 T_{11} - \frac{a_0}{3}\tau_{kk} - \frac{a_1}{3}T_{kk} - \frac{2b_2}{3}\frac{\partial A_1}{\partial x_1}$$

$$- \frac{2b_0}{3}\varepsilon_{11} - \frac{2b_1}{3}E_{11} + \frac{b_2}{3}\frac{\partial A_2}{\partial x_2} + \frac{b_0}{3}\varepsilon_{22} + \frac{b_1}{3}E_{22} = 0,$$

$$\frac{\partial T_{22}}{\partial t} - \frac{1}{3}\frac{\partial T_{kk}}{\partial t} + a_0\tau_{22} + a_1 T_{22} - \frac{a_0}{3}\tau_{kk} - \frac{a_1}{3}T_{kk} - \frac{2b_2}{3}\frac{\partial A_2}{\partial x_2}$$

$$- \frac{2b_0}{3}\varepsilon_{22} - \frac{2b_1}{3}E_{22} + \frac{b_2}{3}\frac{\partial A_1}{\partial x_1} + \frac{b_0}{3}\varepsilon_{11} + \frac{b_1}{3}E_{11} = 0,$$

$$\frac{\partial T_{12}}{\partial t} + a_0\tau_{12} + a_1 T_{12} - \frac{b_2}{2}\frac{\partial A_2}{\partial x_1} - \frac{b_2}{2}\frac{\partial A_1}{\partial x_2} - b_0\varepsilon_{12} - b_1 E_{12} = 0,$$

$$\frac{\partial T_{kk}}{\partial t} + c_0\tau_{kk} + c_1 T_{kk} - d_2\frac{\partial A_1}{\partial x_1} - d_0\varepsilon_{11} - d_1 E_{11} - d_2\frac{\partial A_2}{\partial x_2} - d_0\varepsilon_{22} - d_1 E_{22} = 0, \quad (3.1)$$

where

$$T_{11} = \frac{\partial \tau_{11}}{\partial t}, \qquad T_{22} = \frac{\partial \tau_{22}}{\partial t}, \qquad T_{12} = \frac{\partial \tau_{12}}{\partial t}, \qquad T_{kk} = \frac{\partial \tau_{kk}}{\partial t},$$

$$E_{11} = \frac{\partial \varepsilon_{11}}{\partial t}, \qquad E_{22} = \frac{\partial \varepsilon_{22}}{\partial t}, \qquad E_{12} = \frac{\partial \varepsilon_{12}}{\partial t}, \qquad A_1 = \frac{\partial v_1}{\partial t}, \quad (3.2)$$

$$A_2 = \frac{\partial v_2}{\partial t}, \qquad v_1 = \frac{\partial u_1}{\partial t}, \qquad v_2 = \frac{\partial u_2}{\partial t}.$$

Note that A_1 and A_2 are the particle accelerations in the x_1 and x_2 directions, respectively, and $\tau_{kk} = \tau_{11} + \tau_{22} + \tau_{33}$. Furthermore, one has the following compatibility equations:

$$\frac{\partial E_{11}}{\partial t} - \frac{\partial A_1}{\partial x_1} = 0, \qquad \frac{\partial E_{22}}{\partial t} - \frac{\partial A_2}{\partial x_2} = 0, \qquad \frac{\partial E_{12}}{\partial t} - \frac{1}{2}\left(\frac{\partial A_2}{\partial x_1} + \frac{\partial A_1}{\partial x_2}\right) = 0. \quad (3.3)$$

Equations (2.1) and (3.1)–(3.3) constitute a system of first order governing partial differential equations which can be written in matrix form as

$$\mathbf{A}\mathbf{U}_{,t} + \mathbf{B}\mathbf{U}_{,2} + \mathbf{D}\mathbf{U}_{,1} + \mathbf{F} = 0, \tag{3.4}$$

where

$$\mathbf{A} = \mathbf{I} + \mathbf{a}, \tag{3.5}$$

with $\mathbf{I}$ being a (20×20) identity matrix and $\mathbf{a}$ a (20×20) square matrix whose elements are all zero except

$$a_{14} = a_{24} = -\tfrac{1}{3}. \tag{3.6}$$

In equation (3.4), $\mathbf{B}$ and $\mathbf{D}$ are (20×20) square matrices with the elements all zero except

$$\begin{aligned}
&b_{1(18)} = d_{2(17)} = \frac{b_2}{3}, \qquad b_{2(18)} = d_{1(17)} = \frac{-2b_2}{3},\\
&b_{3(17)} = d_{3(18)} = -\frac{b_2}{2}, \qquad b_{4(18)} = d_{4(17)} = -d_2,\\
&b_{10(18)} = d_{9(17)} = -1, \qquad b_{11(17)} = d_{11(18)} = -\frac{1}{2},\\
&b_{17(3)} = d_{17(1)} = -\frac{1}{\rho}, \qquad b_{18(2)} = d_{(18)3} = -\frac{1}{\rho}.
\end{aligned} \tag{3.7}$$

$\mathbf{F}$ is a 20-dimensional column vector with the elements

$$\begin{aligned}
f_1 &= a_0\tau_{11} + a_1T_{11} - \frac{a_0}{3}\tau_{kk} - \frac{a_1}{3}T_{kk} - \frac{2b_0}{3}\varepsilon_{11} - \frac{2b_1}{3}E_{11} + \frac{b_0}{3}\varepsilon_{22} + \frac{b_1}{3}E_{22},\\
f_2 &= a_0\tau_{22} + a_1T_{22} - \frac{a_0}{3}\tau_{kk} - \frac{a_1}{3}T_{kk} - \frac{2b_0}{3}\varepsilon_{22} - \frac{2b_1}{3}E_{22} + \frac{b_0}{3}\varepsilon_{11} + \frac{b_1}{3}E_{11},\\
f_3 &= a_0\tau_{12} + a_1T_{12} - b_0\varepsilon_{12} - b_1E_{12},\\
f_4 &= c_0\tau_{kk} + c_1T_{kk} - d_0\varepsilon_{11} - d_1E_{11} - d_0\varepsilon_{22} - d_1E_{22},\\
f_5 &= -T_{11}, \qquad f_6 = -T_{22}, \qquad f_7 = -T_{12}, \qquad f_8 = -T_{kk},\\
f_9 &= f_{10} = f_{11} = f_{17} = f_{18} = 0, \qquad f_{12} = -E_{11}, \qquad f_{13} = -E_{22}, \qquad f_{14} = -E_{12},\\
f_{15} &= -A_1, \qquad f_{16} = -A_2, \qquad f_{19} = -v_1, \qquad f_{20} = -v_2,
\end{aligned} \tag{3.8}$$

and $\mathbf{U}$ is a 20-dimensional column vector containing the unknowns,

$$\begin{aligned}
\mathbf{U} = (&T_{11}, T_{22}, T_{12}, T_{kk}, \tau_{11}, \tau_{22}, \tau_{12}, \tau_{kk}, E_{11}, E_{22}, E_{12}, \varepsilon_{11}, \varepsilon_{22}, \varepsilon_{12},\\
&v_1, v_2, A_1, A_2, u_1, u_2)^{\mathrm{T}},
\end{aligned} \tag{3.9}$$

where T designates the transpose. In equation (3.4), a comma denotes partial differentiation: i.e.,

$$\mathbf{U}_{,t} = \frac{\partial \mathbf{U}}{\partial t}, \qquad \mathbf{U}_{,1} = \frac{\partial \mathbf{U}}{\partial x_1}, \qquad \mathbf{U}_{,2} = \frac{\partial \mathbf{U}}{\partial x_2}. \tag{3.10}$$

To apply the numerical technique stated above, one first takes the Fourier transform of the system of governing equations, equation (3.4), with respect to x_1. This eliminates the dependence of the field variables on x_1, and the resulting transformed equations can be written in the form of a system of first order partial differential equations as

$$\mathbf{A}\mathbf{U}^{\mathrm{F}}_{,t} + \mathbf{B}\mathbf{U}^{\mathrm{F}}_{,2} + G = 0, \tag{3.11}$$

where the superscript F stands for the Fourier transform and the vector $\mathbf{G}$ is a 20-dimensional column vector whose elements are

$$g_1 = a_0\tau^{\mathrm{F}}_{11} + a_1 T^{\mathrm{F}}_{11} - \frac{a_0}{3}\tau^{\mathrm{F}}_{kk} - \frac{a_1}{3} T^{\mathrm{F}}_{kk} - \frac{2b_0}{3}\varepsilon^{\mathrm{F}}_{11} - \frac{2b_1}{3} E^{\mathrm{F}}_{11} + \frac{b_0}{3}\varepsilon^{\mathrm{F}}_{22} + \frac{b_1}{3} E^{\mathrm{F}}_{22} - \frac{2b_2}{3}\mathrm{i}kA^{\mathrm{F}}_1,$$

$$g_2 = a_0\tau^{\mathrm{F}}_{22} + a_1 T^{\mathrm{F}}_{22} - \frac{a_0}{3}\tau^{\mathrm{F}}_{kk} - \frac{a_1}{3} T^{\mathrm{F}}_{kk} - \frac{2b_0}{3}\varepsilon^{\mathrm{F}}_{22} - \frac{2b_1}{3} E^{\mathrm{F}}_{22} + \frac{b_0}{3}\varepsilon^{\mathrm{F}}_{11} + \frac{b_1}{3} E^{\mathrm{F}}_{11} + \frac{b_2}{3}\mathrm{i}kA^{\mathrm{F}}_1,$$

$$g_3 = a_0\tau^{\mathrm{F}}_{12} + a_1 T^{\mathrm{F}}_{12} - b_0\varepsilon^{\mathrm{F}}_{12} - b_1 E^{\mathrm{F}}_{12} - \frac{b_2}{2}\mathrm{i}kA^{\mathrm{F}}_2,$$

$$g_4 = c_0\tau^{\mathrm{F}}_{kk} + c_1 T^{\mathrm{F}}_{kk} - d_0\varepsilon^{\mathrm{F}}_{11} - d_1 E^{\mathrm{F}}_{11} - d_0\varepsilon^{\mathrm{F}}_{22} - d_1 E^{\mathrm{F}}_{22} - d_2\mathrm{i}kA^{\mathrm{F}}_1,$$

$$g_5 = -T^{\mathrm{F}}_{11}, \qquad g_6 = -T^{\mathrm{F}}_{22}, \qquad g_7 = -T^{\mathrm{F}}_{12}, \qquad g_8 = -T^{\mathrm{F}}_{kk}, \qquad g_9 = -\mathrm{i}kA^{\mathrm{F}}_1,$$

$$g_{10} = 0, \qquad g_{11} = -\tfrac{1}{2}\mathrm{i}kA^{\mathrm{F}}_2, \qquad g_{12} = -E^{\mathrm{F}}_{11}, \qquad g_{13} = -E^{\mathrm{F}}_{22}, \qquad g_{14} = -E^{\mathrm{F}}_{12},$$

$$g_{15} = -A^{\mathrm{F}}_1, \qquad g_{16} = -A^{\mathrm{F}}_2, \qquad g_{17} = -\frac{1}{\rho}\mathrm{i}kT^{\mathrm{F}}_{11}, \qquad g_{18} = -\frac{1}{\rho}\mathrm{i}kT^{\mathrm{F}}_{12},$$

$$g_{19} = -v^{\mathrm{F}}_1, \qquad g_{20} = -v^{\mathrm{F}}_2. \tag{3.12}$$

In equations (3.12), i is the imaginary number and k is the Fourier transform parameter which corresponds to the wave number for the x_1 direction.

The Fourier transforms of the boundary conditions, equations (2.10)–(2.13), with respect to x_1 gives, at $x_2 = 0$,

$$\tau^{\mathrm{F}}_{22}(k, 0, t) = -p^{\mathrm{F}}(k, t), \qquad \tau^{\mathrm{F}}_{12}(k, 0, t) = 0 \tag{3.13}$$

or

$$\tau^{\mathrm{F}}_{12}(k, 0, t) = -s^{\mathrm{F}}(k, t), \qquad \tau^{\mathrm{F}}_{22}(k, 0, t) = 0 \tag{3.14}$$

and, at $x_2 = H$,

$$\tau^{\mathrm{F}}_{22}(k, H, t) = 0, \qquad \tau^{\mathrm{F}}_{12}(k, H, t) = 0 \tag{3.15}$$

or

$$u_1^{\mathrm{F}}(k, H, t) = 0, \qquad u_2^{\mathrm{F}}(k, H, t) = 0. \tag{3.16}$$

The Fourier transforms of the interface conditions require that the transformed stresses τ_{22}^{F}, τ_{12}^{F} and the transformed displacements $u_1^{\mathrm{F}}, u_2^{\mathrm{F}}$ be continuous across the interfaces of the layers. The quiescent initial conditions imply that all the transformed field variables are zero at $t = 0$. The formulation of the problem in the Fourier transform space is now complete.

The second step of the procedure involves the determination of the solution in transform space, which requires the solutions of equations (3.11) for each layer satisfying the boundary conditions, equations (3.13)–(3.16), at the boundaries, the interface conditions at the interfaces and the zero initial conditions. The system of governing equations, equations (3.11), is hyperbolic, and the solution for a given value of the wave number (transform parameter) k is constructed by employing the method of characteristics. In the method of characteristics, the system of governing hyperbolic partial differential equations is transformed into a system of ordinary differential equations, each of which is valid along a different family of characteristic lines. These equations, called the canonical equations, are suitable to obtain the solution numerically by a step-by-step integration procedure in such a way that the domain of dependence be preserved at the points of the solution domain. The convergence and numerical stability of the method are well established; see the books by Courant and Hilbert [45] and Whitham [46]. The details of the method of characteristics can be found in references [45, 46]. The way it is applied in this study is, however, closer to that applied by McNiven and Mengi [47].

The characteristic lines, along which the canonical equations are valid, are governed by the characteristic equation

$$\det(\mathbf{B} - V\mathbf{A}) = 0, \tag{3.17}$$

where $V = \mathrm{d}x_2/\mathrm{d}t$. Equation (3.17) yields the eigenvalues $V_i (i = 1\text{–}20)$, which are

$$V_1 = c_p, \qquad V_2 = -c_p, \qquad V_3 = c_s, \qquad V_4 = -c_s, \qquad V_i = 0 \qquad (i = 5\text{–}20), \tag{3.18}$$

where

$$c_p = \left[\frac{1}{3\rho}(2b_2 + d_2)\right]^{1/2} = \left(\frac{\lambda + 2\mu}{\rho}\right)^{1/2}, \qquad c_s = \left[\frac{b_2}{2\rho}\right]^{1/2} = (\mu/\rho)^{1/2}. \tag{3.19}$$

The characteristic manifold is thus composed of families of straight lines $\mathrm{d}x_2/\mathrm{d}t = V_i$ $(i = 1\text{–}20)$. $\mathrm{d}x_2/\mathrm{d}t = V_1 = c_p$ and $\mathrm{d}x_2/\mathrm{d}t = V_2 = -c_p$ describe two characteristic families of straight lines with slopes (c_p) and $(-c_p)$, respectively, on the $(x_2 - t)$ plane. $\mathrm{d}x_2/\mathrm{d}t = V_3 = c_s$ and $\mathrm{d}x_2/\mathrm{d}t = V_4 = -c_s$ describe another two families of straight lines with the slopes (c_s) and $(-c_s)$, whereas, $\mathrm{d}x_2/\mathrm{d}t = V_i$ $(i = 5\text{–}20)$ define straight lines parallel to the t-axis; see Figure 2.

The canonical equations are determined from

$$\mathbf{l}_i^{\mathrm{T}}\mathbf{A}\frac{\mathrm{d}\mathbf{U}^{\mathrm{F}}}{\mathrm{d}t} + \mathbf{l}_i^{\mathrm{T}}\mathbf{G} = 0, \tag{3.20}$$

which holds along $\mathrm{d}x_2/\mathrm{d}t = V_i$ $(i = 1\text{–}20)$. In equation (3.20), $\mathrm{d}/\mathrm{d}t$ denotes the total time derivative along a characteristic line and $\mathbf{l}_i$ is the left-hand eigenvector satisfying the

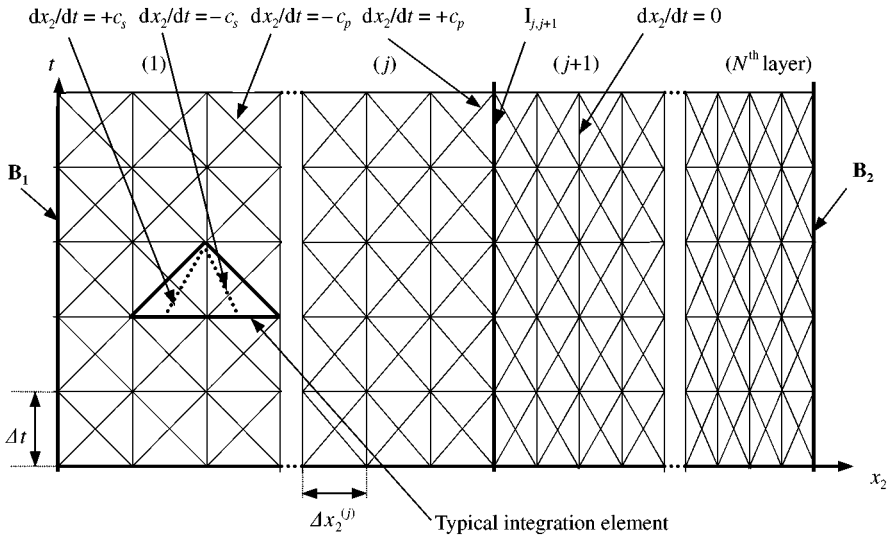

Figure 2. Network of characteristic lines on the $(x_2 - t)$ plane.

equation

$$\mathbf{B}^{\mathrm{T}}\mathbf{l}_i = V_i\mathbf{A}^{\mathrm{T}}\mathbf{l}_i. \tag{3.21}$$

In view of equations (3.5)–(3.7) and (3.18), the left-hand eigenvectors can be determined from equation (3.21). When these left-hand eigenvectors together with **A** and **G** defined in equations (3.5), (3.6) and (3.12) are substituted into equation (3.20), the canonical equations can be obtained explicitly.

For a given value of k, these canonical equations can be integrated easily by using the network shown in Figure 2, which is composed of characteristic lines for the N different layers. In this integration procedure, one uses the boundary conditions, equations (3.13)–(3.16), along the boundary lines $\mathbf{B}_1$ and $\mathbf{B}_2$, the interface conditions along the interface lines $I_{j,j+1}$ ($\mathrm{j} = 1, \ldots, N-1$), denoting the interface between the j th and $(j+1)$th layers, and zero initial conditions at $t = 0$. The numerical procedure is started from the x_2-axis of the $(x_2 - t)$ plane.

Finally, one inverts numerically the solution obtained in the Fourier space back into real space by employing the inverse Fourier transform formula. This requires the construction of the solution in the characteristic plane at the discrete wave number points $(k_0, k_1, k_2, \ldots)$ with an increment Δk. The number of wave number points and the cut-off value of k to be considered in the analysis should be chosen properly, since they play an important role in achieving a desired accuracy in the solution. The inversion is performed conveniently by using the fast Fourier transform (FFT) algorithm [48, 49]. It may be noted that the same algorithm is also used for computing the Fourier transforms $p^{\mathrm{F}}(k, t)$ and $s^{\mathrm{F}}(k, t)$ of the applied surface tractions.

4. NUMERICAL RESULTS AND DISCUSSIONS

First, several examples will be given to verify the validity of the numerical technique employed in this study. The first example is the so-called Lamb's problem whose analytical

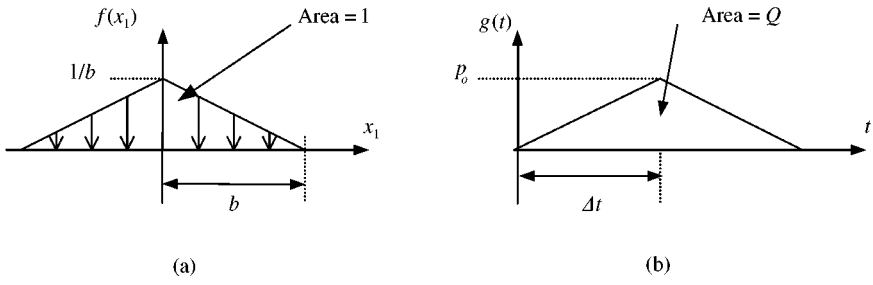

Figure 3. (a) Triangular load on half-space. (b) Time variation of the applied load.

treatment was given by Lamb [50]. Lamb presented the solution for the horizontal surface displacement up to the arrival of the S wave; whereas, for the vertical displacement, the complete solution was given. Numerical treatment of this problem by employing the time-domain boundary element method was given by Israel and Banerjee [51].

The elastic half-space (HS) is subjected to surface tractions whose spatial and temporal distributions are triangular in the form shown in Figure 3, where $f(x_1)g(t)$ represents the applied traction "p" in this and other examples of verification. The triangular spatial and temporal distributions are chosen to simulate a line load and a delta pulse in time. The solution for this elastic half-space (HS) problem by the present method is obtained as a special case of the general multilayered viscoelastic problem by suitably choosing the material properties and the geometric parameters. The surface displacements due to the vertical applied line load obtained by the present method at two different locations are presented in Figure 4 together with Lamb's solution. The normalization parameters used are: x, the distance from the mid-point of the region over which the surface tractions are applied; μ, the shear modulus of the HS; c_p and c_s, the propagation velocities of the P and S waves; and Q, the magnitude of the triangular pulse, i.e., the area under the curve in Figure 3(b). Here, note that as the point gets away from the region of applied surface tractions, i.e., as (x/b) increases, and as Δt gets smaller, the results converge towards Lamb's solution, which is the consequence of the fact that, with increasing distance and decreasing Δt, the load approaches a line load in space and a delta pulse in time. One can further note that the curves in Figure 4 are very close to those given in reference [51], where the spatial distribution was taken to be parabolic.

Now, a remark regarding the results in Figure 4 is in order. Lamb's solution contains a jump at the wave front (which corresponds to the arrival of P waves); but, our solution smooths out that jump. To explain this discrepancy, we note that the time and spatial variations of the line load in Lamb's problem are Dirac delta functions. On the other hand, in the present study these variations are taken as triangular as shown in Figure 3, which, we think, smooths out the jump. We believe that the above-mentioned discrepancy stems from the approximation of the time and spatial variations of the pulse, not from the method. In fact, the 1-D problem which will be considered shortly shows that the method presented in this study could predict the sharp variations at the wave front very well.

The second example for verification is an elastic HS subjected to suddenly applied normal surface tractions at $t = 0$ with a trapezoidal distribution in the x_1 direction and a step function with an initial ramp in time, see Figure 5. The HS is initially at rest. The loading is defined by $a = 12{\cdot}2$ m, $b = 10{\cdot}67$ m and $p_0 = 6891{\cdot}2$ kN/m^2 with a rise time of $t_r = 20 \times 10^{-3}$ s. The elastic constants of the HS are $\mu = 599{\cdot}6$ MPa and $\lambda = 257$ MPa. The dilatational and shear wave velocities are $c_p = 835{\cdot}2$ m/s and $c_s = 535{\cdot}9$ m/s. The curves for the vertical displacement at the interior point G (45·74 , 3·05 m) and the normal stress τ_{22} at

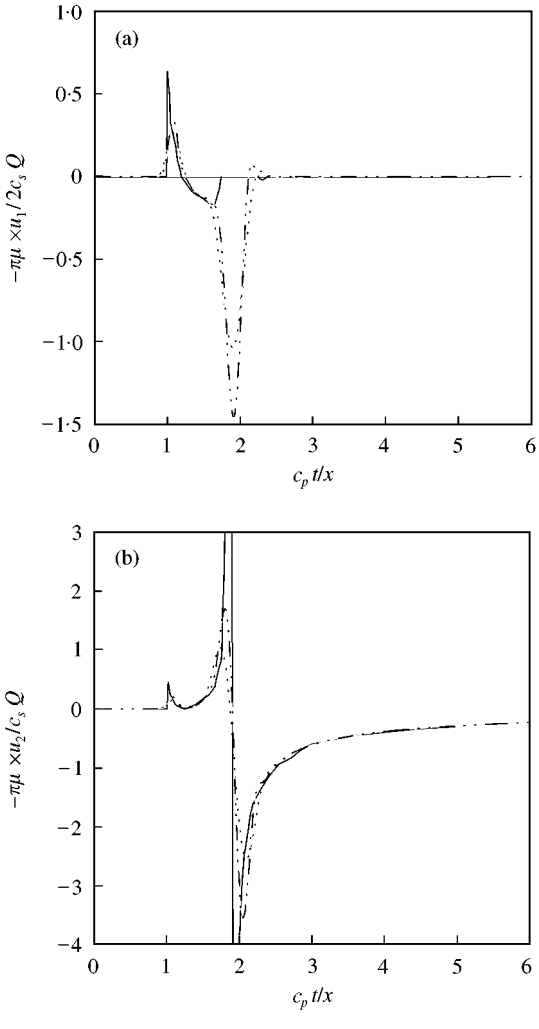

Figure 4. Displacement at the surface of the HS. (a) Horizontal displacement. (b) Vertical displacement ——, Lamb's Solution; – – – – –, $(x/b) = 6$; – – – –, $(x/b) = 9$.

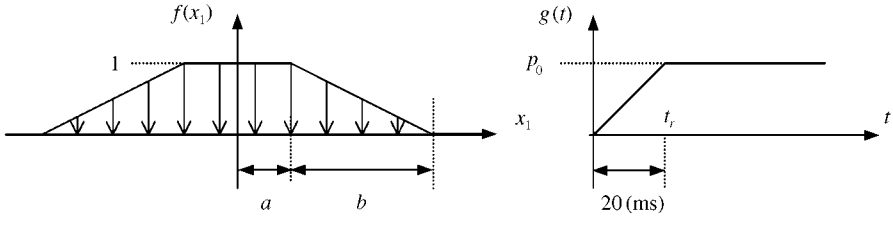

Figure 5. Space and time variations of the load applied on a half-space.

point B (22·86, 22·86 m) obtained by the present method as a special case of the general formulation for multilayered viscoelastic media are given in Figures 6 and 7 respectively. The results obtained previously by Israil and Banerjee [52] and Birgissan and Crouch [53]

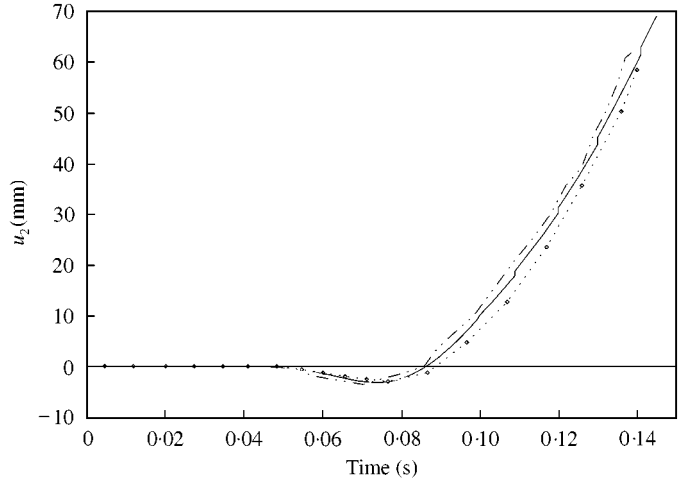

Figure 6 Time variation of the vertical displacement at point G(45·74, 3·05 m). ——, Present; – –◇– –, Israil & Banerjee; – – – –, Birgisson & Crouch.

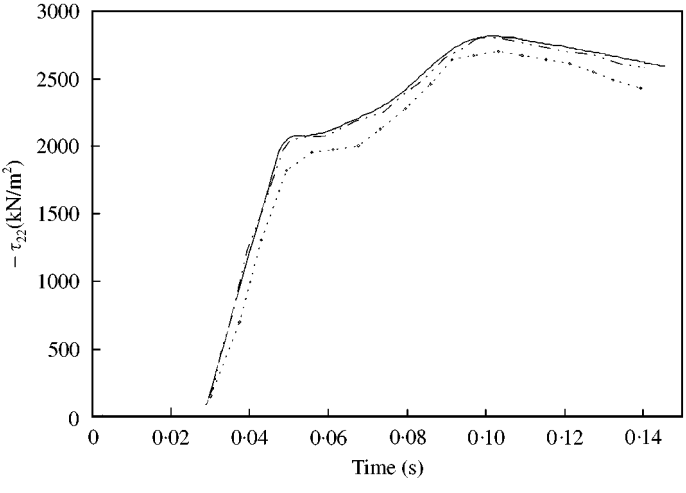

Figure 7. Time variation of τ_{22} at point B(22·86, 22.86 m). ——, Present; – –◇– –, Israil & Banerjee; – – – –, Birgisson & Crouch.

by employing a time-domain direct boundary element method are also presented in Figures 6 and 7. Very good agreement is observed between the curves.

The next example of verification involves an elastic layer overlaying an elastic HS with different shear moduli μ_1 and μ_2, all other properties remaining the same. The portion of the top surface of width $2b$ is subjected to a uniform load with the triangular pulse in time as shown in Figure 8. The depth of the upper layer is $H = 3b$. The rise time of the pulse is $t_r = 0{\cdot}5437b/c_s$, where c_s is the shear-wave velocity in the upper layer. Three different cases are studied with the ratios of shear moduli: $\mu_1/\mu_2 = 1$, 0·5, and 0.25. The vertical displacements at the location P($x_1/b = 5, x_2 = 0$) obtained by the present analysis are given in Figure 9. The corresponding solutions obtained by the time-domain boundary element method [51] are also presented in Figure 9, showing a good agreement between the curves found by the two different methods.

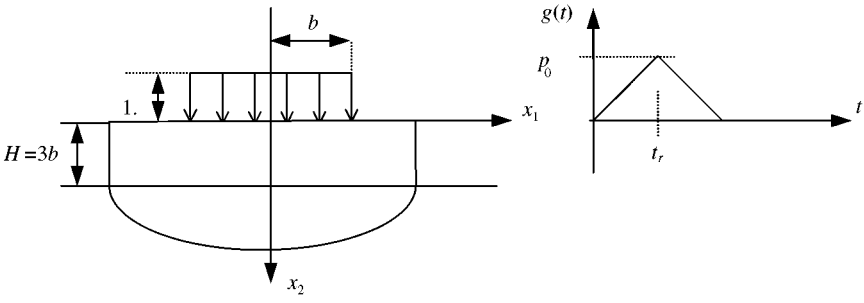

Figure 8. Space and time variations of the load applied on a layer overlaying a half-space.

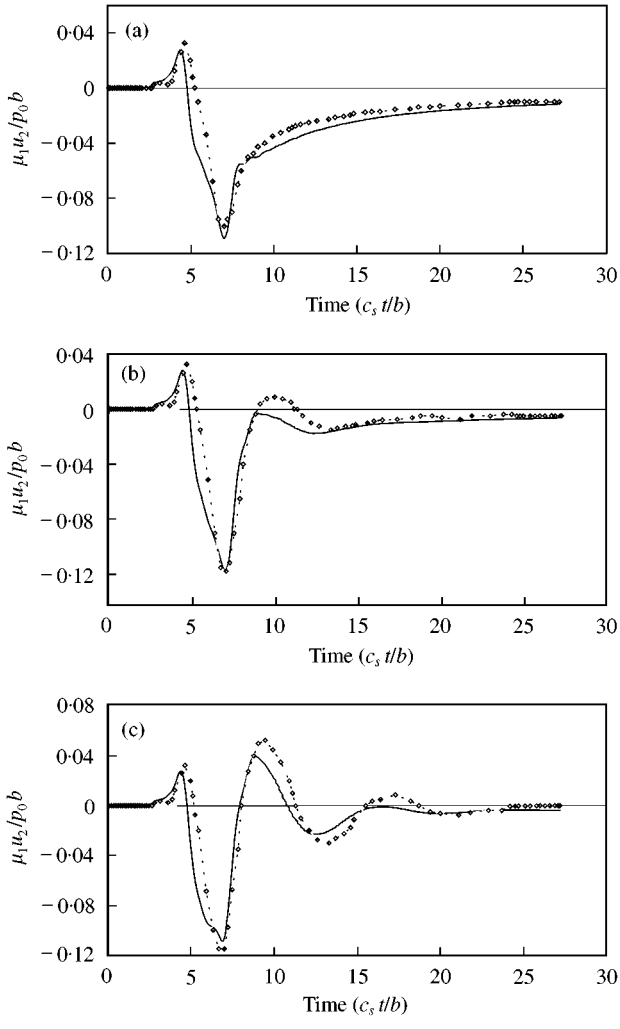

Figure 9. Time variations of the vertical displacements at point P ($x_1/b = 5$, $x_2 = 0$) for different ratios of shear moduli. (a) $\mu_1/\mu_2 = 1$; (b) $\mu_1/\mu_2 = 0{\cdot}5$; (c) $\mu_1/\mu_2 = 0{\cdot}25$. ——, Present; – –◇– –, BEM.

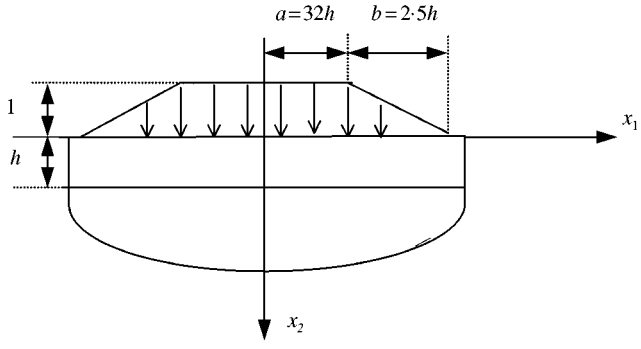

Figure 10. Space variation of the load applied on a viscoelastic layer overlaying an elastic half-space.

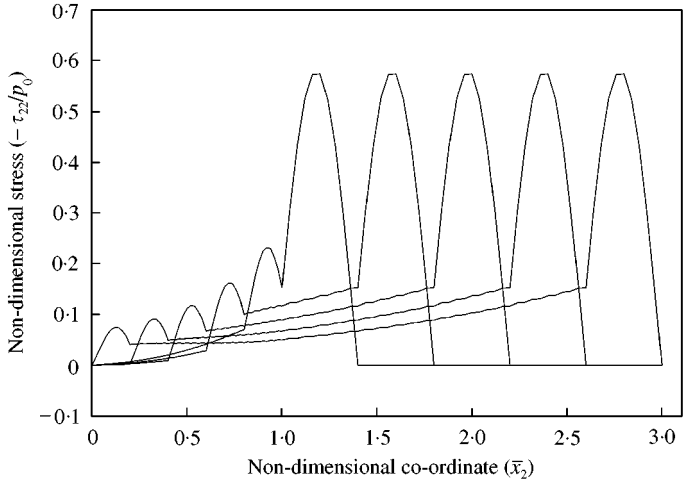

Figure 11. Space variations of the normal stress (τ_{22}/p_0) at non-dimensional times $\bar{t} = 1{\cdot}2$, $1{\cdot}4$, $1{\cdot}6$, $1{\cdot}8$ and $2{\cdot}0$.

In the last example of verification, a viscoelastic layer overlaying an elastic HS is considered. The viscoelastic layer is modelled as a standard linear solid, i.e., $n = 1$ is taken in equations (2.3) and (2.6). The top surface of the viscoelastic layer is subjected to normal surface tractions with a trapezoidal distribution in the x_1 direction and a half-sine pulse, $g(t) = p_0 \sin(5\pi t)\mathrm{H}(t)\mathrm{H}(0{\cdot}2 - t)$, in time: see Figure 10. The width of the applied load, $a = 32h$ and $b = 2{\cdot}5\,h$, is taken much larger than the depth of the top layer, so that the two-dimensional solution can simulate a one-dimensional solution where the whole top surface is subjected to uniform surface tractions. The viscoelastic properties of the top layer are taken as $\alpha_0^{(1)} = \alpha_1^{(1)} = \beta_0^{(1)} = \beta_1^{(1)} = 0{\cdot}5$ and $\tau_1^{(1)} = \zeta_1^{(1)} = 0{\cdot}25$, where the superscripts 1 in parentheses imply that the corresponding quantities pertain to layer 1, the upper layer. The bottom HS characterized by the superscript 2, is assumed to be elastic with $\alpha_0^{(2)} = \beta_0^{(2)} = 1{\cdot}0$ and $c_p^{(2)} = 2c_p^{(1)}$. Since our analysis is two-dimensional, we should also have shear-wave velocities, which are chosen as $c_s^{(1)} = \sqrt{1/3}\,c_p^{(1)}$ and $c_s^{(2)} = \sqrt{2/3}\,c_p^{(1)}$. The variations of the non-dimensional normal stress τ_{22}/p_0 with position $\bar{x}_2 = x_2/h$ at different times is presented in Figure 11. The same problem was solved by Jiang and Haddow [32] by a finite element method and method of characteristics as a one-dimensional problem; their results coincide with those displayed in Figure 11. There is perfect agreement between the two solutions.

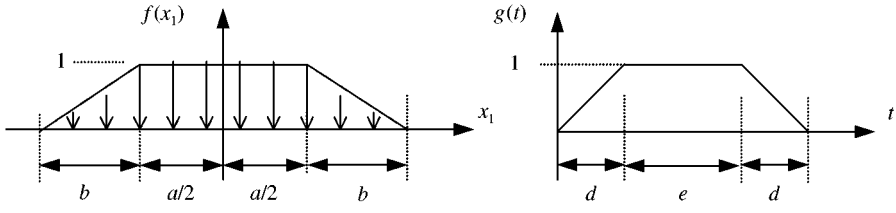

Figure 12. Space and time variations of the surface tractions applied on the top surface of the multilayered media.

We now present some results for multilayered viscoelastic media with two discrete relaxation times, i.e., $n = 2$ is taken in equations (2.3) and (2.6). In the numerical computations, the top surface is assumed to be subjected to normal surface tractions and the bottom surface is fixed, i.e., the boundary conditions are as given by equations (2.10) and (2.13). Furthermore, the time and x_1 variations of $p(x_1, t)$ are taken in the form

$$p = p_0 f(x_1) g(t), \tag{4.1}$$

where p_0 is the intensity of the applied normal stresses, and the functions $f(x_1)$ and $g(t)$ describe trapezoidal distributions with respect to x_1 and t, respectively, as shown in Figure 12. The function $g(t)$ has a finite time duration $(e + 2d)$. Spacewise, f is a strip load of the width $(a + 2b)$ acting between the points $x_1 = \mp (a/2 + b)$. The "e" and "d" values (see Figure 12) are chosen to be

$$e = 0{\cdot}4T, \qquad d = 0{\cdot}2T, \tag{4.2}$$

where T is a characteristic time defined by $T = h/c_s^{(1)}$ in which h is a characteristic length and $c_s^{(1)}$ is the shear-wave velocity pertaining to the top layer.

Two different sets of values are assigned to a and b (see Figure 12). The first one is

$$a = 2h, \qquad b = 0{\cdot}5h, \tag{4.3}$$

for which the width of the strip load becomes comparable with the characteristic length. The second set is

$$a = 20h, \qquad b = 5h, \tag{4.4}$$

which corresponds to the case in which the width of the strip load becomes very large compared to the characteristic length.

The numerical computations have been carried out and the results are displayed in terms of non-dimensional quantities. These dimensionless quantities are defined as

$$\bar{x}_i = \frac{x_i}{h}, \qquad \bar{t} = \frac{t c_s^{(1)}}{h}, \qquad \bar{\rho}_j = \frac{\rho_j}{\rho_1},$$

$$(\bar{\tau}_{11}, \bar{\tau}_{22}, \bar{\tau}_{12}) = \frac{1}{\mu_1}(\tau_{11}, \tau_{22}, \tau_{12}), \qquad \bar{c}_p^{(j)} = \frac{c_p^{(j)}}{c_s^{(1)}},$$

$$\bar{c}_s^{(j)} = \frac{c_s^{(j)}}{c_s^{(1)}}, \qquad \bar{\mu}_j = \frac{\mu_j}{\mu_1}, \qquad \bar{\lambda}_j = \frac{\lambda_j}{\mu_1},$$

$$(\bar{\tau}_m^{(j)}, \bar{\zeta}_m^{(j)}) = \frac{c_s^{(1)}}{h}(\tau_m^{(j)}, \zeta_m^{(j)}) \quad (m = 1, 2),$$

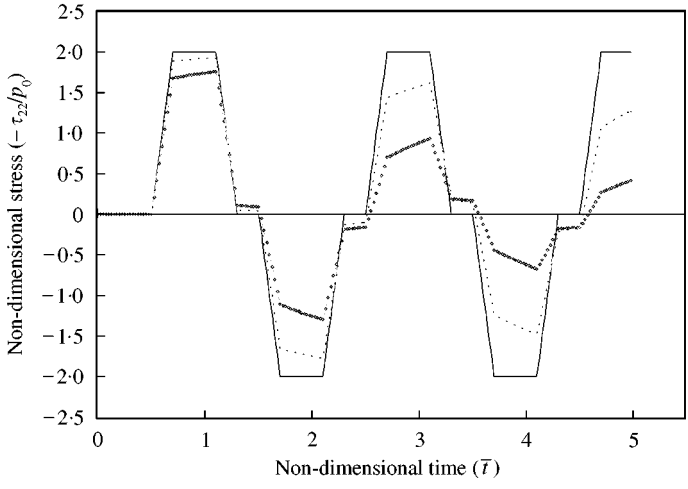

Figure 13. Time variation of the normal stress (τ_{22}/p_0) at $\bar{x}_1 = 0, \bar{x}_2 = 1$ when the width of the strip load is very large compared to the thickness of the laminate. ——, Elastic; - - - - -, viscoelastic 1; – –◇– –, viscoelastic 2.

$$\bar{u}_i^{(j)} = \frac{u_i^{(j)}}{h}, \quad \bar{v}_i^{(j)} = \frac{v_i^{(j)}}{c_s^{(1)}}, \qquad \bar{A}_i^{(j)} = \frac{A_i^{(j)} h}{(c_s^{(1)})^2}, \quad (i = 1 - 2; j = 1, 2, 3, \ldots, N), \tag{4.5}$$

where the non-dimensional quantities are designated by bars. The subscript j or the superscript j in parentheses denotes the quantity belonging to the jth layer. Furthermore, $\rho_1, \mu_1, c_s^{(1)}$ are the mass density, impact shear modulus and shear-wave velocity of the top layer respectively. In the computations, the intensity of the applied normal stress is chosen as $\bar{p}_0 = p_0/\mu_1 = 1$.

In Figure 13, the variation of the dimensionless normal stress τ_{22}/p_0 with time $\bar{t}$ at the location $\bar{x}_1 = 0, \bar{x}_2 = 1{\cdot}0$ of a multilayered medium consisting of four layers is shown. The characteristic length h in this example is chosen as the thickness of the multilayered medium. The surface pressure is defined by equations (4.1) (4.2) and (4.4), implying that the width of the strip load is very large compared to the laminate thickness. The thicknesses and material properties of the four layers are assumed to be the same. Two sets of material properties are assumed for the layers of the viscoelastic laminate. The first set is

$$\alpha_0 = \beta_0 = 0{\cdot}8, \qquad \alpha_1 = \alpha_2 = \beta_1 = \beta_2 = 0{\cdot}1, \qquad \bar{\tau}_1 = \bar{\zeta}_1 = 1, \quad \bar{\tau}_2 = \bar{\zeta}_2 = 2. \tag{4.6}$$

The second set is selected as

$$\alpha_0 = \beta_0 = 0{\cdot}4, \qquad \alpha_1 = \alpha_2 = \beta_1 = \beta_2 = 0{\cdot}3, \qquad \bar{\tau}_1 = \bar{\zeta}_1 = 1, \quad \bar{\tau}_2 = \bar{\zeta}_2 = 2. \tag{4.7}$$

For both sets, we choose

$$\bar{\lambda} = 2. \tag{4.8}$$

Note that, in view of the non-dimensionalization we are using in the study, we also have

$$\bar{\mu} = 1, \qquad \bar{\rho} = 1, \qquad \bar{h}_i = h_i/h = 0{\cdot}25 \quad (i = 1 - 4) \tag{4.9}$$

As the material properties of all four layers are taken to be same, the curves in Figure 13 represent solutions for a single elastic or viscoelastic layer with a non-dimensional thickness $\bar{H} = 1$. Since the width of the applied load is very large compared to the thickness of the

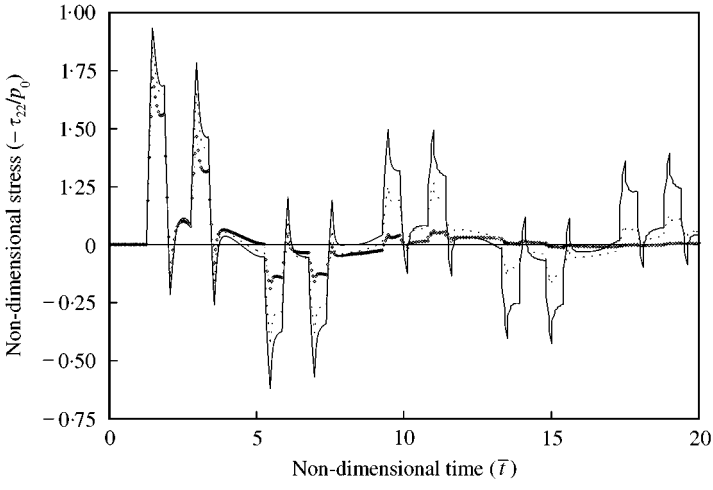

Figure 14. Time variation of the normal stress (τ_{22}/p_0) at $\bar{x}_1 = 0$, $\bar{x}_2 = 1$ for $a = 2h$, $b = 0{\cdot}5h$. ——, Elastic; - - - - -, viscoelastic 1; – –◇– –, viscoelastic 2.

layer, the problem is approximately one-dimensional, for which the exact elasticity solution is available. The elastic solution in Figure 13 is obtained by treating the problem as two-dimensional, which agrees very well with the exact. This provides further confidence about the accuracy of the numerical technique used in the study. The curves for the viscoelastic materials 1 and 2 clearly display, in the wave profiles, the effects of viscous damping, which is more pronounced for material 2.

In Figure 14, the variation of τ_{22}/p_0 with time $\bar{t}$ at the location $\bar{x}_1 = 0$, $\bar{x}_2 = 1{\cdot}0$ of a single layer is displayed. In this example, the characteristic length h is chosen as one-fourth of the layer thickness, i.e., $h = H/4$. Two sets of material properties as defined by equations (4.6)–(4.8) are assumed for the viscoelastic layer. The time and x_1-distributions of the strip load applied at the top surface is chosen as given by equations (4.1)–(4.3). Note that the width of the applied strip load in this case is comparable with the layer thickness. The elastic solution is also given in Figure 14 for comparison. The curves of Figure 14 clearly show the effects of reflections at the top and bottom surfaces through the sudden changes in the stress levels. The sharp variations at the wave fronts are properly accounted for. The attenuation in the wave profiles due to viscous damping, more pronounced for smaller values of α_0 and β_0, is apparent in the curves. The damping effects become dominant for large times. Furthermore, in Figure 14, the scattering and radiation effects may be clearly observed, which are due to inclined waves reflected at layer boundaries. This is more apparent in the elastic case, in which the stress peak values decrease as time increases.

The time variations of the non-dimensional stress τ_{22}/p_0 and displacement $\bar{u}_2$ with time $\bar{t}$ at different locations of multilayered viscoelastic media consisting of four layers are displayed in Figures 15–17. The multilayered media consist of two pairs of alternating layers, denoted as layers 1 and 2, with the layer sequence, starting from the top, as 1/2/1/2. All the layers have equal thicknesses. The characteristic length h used in non-dimensionalization is taken as equal to the layer thickness. Two different multilayered viscoelastic media, named as I and II, are considered. For medium I, layers 1 and 2 have the same viscoelastic properties which are given by equation (4.6). Furthermore, we have $\bar{h}_i = h_i/h = 1$ and choose $\bar{\rho}_i = 1$, $\bar{\lambda}_i = 2$ $(i = 1 - 2)$ for both layers. The only difference between the layers is that we take $\bar{\mu}_1 = 1$ and $\bar{\mu}_2 = 2$. For medium II, all the properties are the same as laminate I except that the viscoelastic material properties are now given by

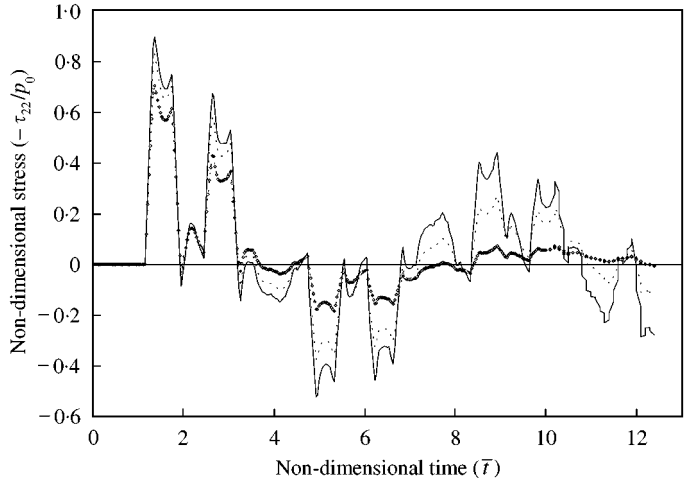

Figure 15. Time variation of the normal stress (τ_{22}/p_0) at $\bar{x}_1 = 0$, $\bar{x}_2 = 2{\cdot}5$ for the multilayered media with two pairs of alternating layers. ——, Elastic; - - - - -, viscoelastic I; – –◆– –, viscoelastic II.

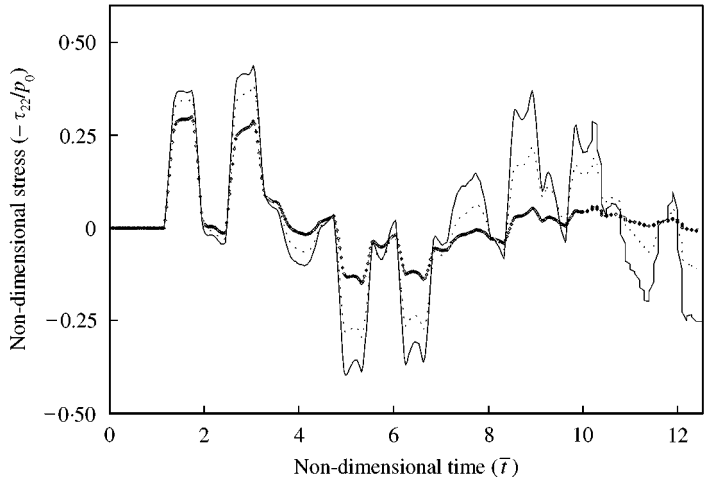

Figure 16. Time variation of the normal stress (τ_{22}/p_0) at $\bar{x}_1 = 1{\cdot}6$, $\bar{x}_2 = 2{\cdot}5$ for the multilayered media with two pairs of alternating layers. ——, Elastic; - - - - -, viscoelastic I; – –◆– –, viscoelastic II.

equation (4.7). The top surfaces of the laminates are subjected to normal strip loads whose time and x_1-distributions are defined by equations (4.1)–(4.3). For the elastic case, the two multilayered media reduce to the same laminate in which $\bar{h}_i = 1$, $\bar{\rho}_i = 1$, $\bar{\lambda}_i = 2$ ($i = 1$–2) and $\bar{\mu}_1 = 1$, $\bar{\mu}_2 = 2$ for the layers 1 and 2 of the laminate. The width of the strip load in this problem is comparable with the thickness of the laminate. The curves of Figure 15 denoting the time variations of τ_{22}/p_0 at the location ($\bar{x}_1 = 0$, $\bar{x}_2 = 2{\cdot}5$) clearly display the effects of reflections from the top and bottom surfaces, reflections and refractions from the interfaces of the layers and the effects of viscous damping. Damping is more dominant in viscoelastic laminate II. The normal stress τ_{22}/p_0 basically dies out for $\bar{t} > 16$ for viscoelastic laminate II. The sharp variations in the stress levels for the elastic laminate are gradually smoothed out by viscous damping in the case of viscoelastic laminates, more distinct for laminate II and for large times. In Figure 16, the time variation of τ_{22}/p_0 at the location ($\bar{x}_1 = 1{\cdot}6$,

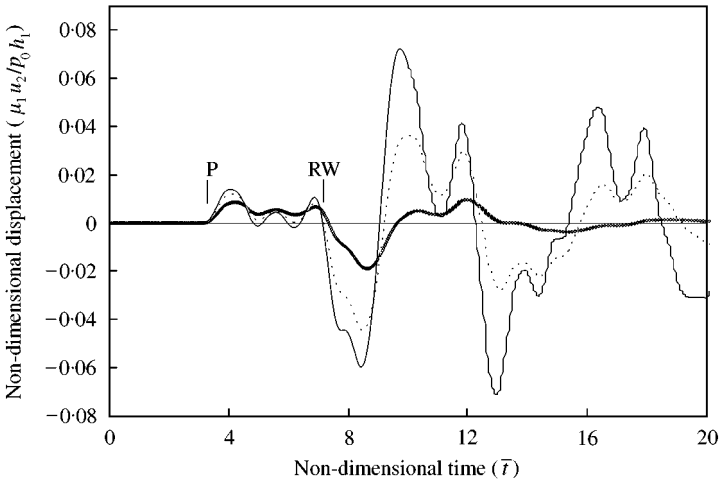

Figure 17. Time variation of the vertical displacement ($\mu_1 u_2/p_0 h_1$) at $\bar{x}_1 = 7{\cdot}5$, $\bar{x}_2 = 0$ for the multilayered media with two pairs of alternating layers. ——, Elastic; - - - - -, viscoelastic I; – –◆– –, viscoelastic II.

$\bar{x}_2 = 2{\cdot}5$) is shown. The curves in this figure exhibit similar trends; the stress peak values, however, are smaller due to the location of the observation point.

Finally, in Figure 17, the variations of the dimensionless displacement component $\bar{u}_2$ with time $\bar{t}$ at the location A ($\bar{x}_1 = 7{\cdot}5$, $\bar{x}_2 = 0$) are shown. Note that the point A is on the top surface and away from the loading region. From the figure one can see that the point A is first disturbed from the rest at the time of arrival of the dilatational P wave. Then, a sharp significant change occurs in the displacement at a later time, denoted by point RW, which can be interpreted as due to the arrival of surface waves. Similar trends observed in Figures 15 and 16 due to reflections, refractions and viscous damping are displayed in these curves as well.

REFERENCES

1. W. M. Ewing, W. S. Jardetsky and F. Press 1957 *Elastic Waves in Layered Media*. New York: McGraw-Hill.
2. L. M. Brekhovskikh 1960 *Waves in Layered Media*. New York: Academic Press.
3. C. T. Sun, J. D. Achenbach and G. Herrmann 1968 *American Society of Mechanical Engineers Journal of Applied Mechanics* **35**, 467–475. Continuum theory for a laminated medium.
4. J. D. Achenbach, C. T. Sun and G. Herrmann 1968 *American Society of Mechanical Engineers Journal of Applied Mechanics* **35**, 689–696. On the vibrations of a laminated body.
5. Y. Mengi 1980 *International Journal of Solids and Structures* **16**, 1155–1168. A new approach for developing dynamic theories for structural elements Part 1. Application to thermoelastic plates.
6. Y. Mengi, G. A. Birlik and H. D. McNiven 1980 *International Journal of Solids and Structures* **16**, 1169–1186. A new approach for developing dynamic theories for structural elements Part 2. Application to thermoelastic layered composites.
7. F. Santosa and W. W. Symes 1991 *SIAM Journal of Applied Mathematics* **51**, 984–1005. A dispersive effective medium for wave propagation in periodic composites.
8. C. T. Sun, J. D. Achenbach and G. Herrmann 1968 *American Society of Mechanical Engineers Journal of Applied Mechanics* **35**, 408–411. Time-harmonic waves in a stratified medium propagating in the direction of the layering.
9. T. J. Delph, G. Herrmann and R. K. Kaul 1979 *American Society of Mechanical Engineers Journal of Applied Mechanics* **46**, 113–119. Harmonic wave propagation in a periodically layered infinite elastic body: plane strain, analytical results.

10. T. J. DELPH, G. HERRMANN and R. K. KAUL 1980 *American Society of Mechanical Engineers Journal of Applied Mechanics* **47**, 531–537. Harmonic wave propagation in a periodically layered infinite elastic body: plane strain, numerical results.
11. A. M. B. BRAGA and G. HERRMANN 1992 *Journal of the Acoustical Society of America* **91**, 1211–1227. Floquet waves in anisotropic periodically layered composites.
12. G. R. LIU, J. TANI, K. WATANABE and T. OHYOSHI 1990 *American Society of Mechanical Engineers Journal of Applied Mechanics* **57**, 923–929. Lamb wave propagation in anisotropic laminates.
13. C. CETINKAYA and A. F. VAKAKIS 1995 *Journal of Sound and Vibration* **182**, 283–302. Transient axisymmetric stress wave propagation in weakly coupled layered structures.
14. C. CETINKAYA, J. BROWN, A. A. F. MOHAMMAD and A. F. VAKAKIS 1997 *International Journal for Numerical Methods in Engineering* **40**, 1639–1665. Near field transient axisymmetric waves in layered structures: effects of weak coupling.
15. S. A. RIZZI and J. F. DOYLE 1992 *Journal of Vibration and Acoustics* **114**, 569–577. A spectral element approach to wave motion in layered solids.
16. T. KUNDU and A. K. MAL 1985 *Wave Motion* **7**, 459–471. Elastic waves in a multilayered solid due to a dislocation source.
17. A. K. MAL 1988 *Wave Motion* **10**, 257–266. Wave propagation in layered composite laminates under periodic surface loads.
18. A. K. MAL and S. S. LIH 1992 *American Society of Mechanical Engineers Journal of Applied Mechanics* **59**, 878–886. Elastodynamic response of a unidirectional composite laminate to concentrated surface loads. Part I.
19. S.-S. LIH and A. K. MAL 1992 *American Society of Mechanical Engineers Journal of Applied Mechanics* **59**, 887–892. Elastodynamic response of a unidirectional composite laminate to concentrated surface loads. Part II.
20. S.-S. LIH and A. K. MAL 1996 *Composites Part B* **27B**, 633–641. Response of multilayered composite laminates to dynamic surface loads.
21. Z. JIANFENG and L. YOUMING 1997 *Wave Motion* **25**, 109–125. Numerical simulation of elastic wave propagation in inhomogeneous media.
22. G. R. LIU, J. TANI, T. OHYOSHI and K. WATANABE 1991 *Journal of Vibration and Acoustics* **113**, 230–234. Transient waves in anisotropic plates, Part I. Theory.
23. G. R. LIU, J. TANI, T. OHYOSHI and K. WATANABE 1991 *Journal of Vibration and Acoustics* **113**, 235–239. Transient waves in anisotropic laminated plates, Part 2. Application.
24. M. TYGEL and P. HUBRAL 1987 *Transient Waves in Layered Media*. Amsterdam: Elsevier Press.
25. J. D. ACHENBACH 1987 *Wave Propagation in Elastic Solids*. New York: North-Holland.
26. J. MIKLOWITZ 1984 *The Theory of Elastic Waves and Wave Guides*. New York: North- Holland.
27. A. H. NAYFEH 1995 *Wave Propagation in Layered Anisotropic Media*. Amsterdam: North-Holland.
28. J. H. M. T. VAN DER HIJDEN 1987 *Propagation of Transient Elastic Waves in Stratified Anisotropic Media*. Amsterdam: North-Holland.
29. T. C. T. TING and I. MUKUNOKI 1979 *American Society of Mechanical Engineers Journal of Applied Mechanics* **46**, 329–336. A theory of viscoelastic analogy for wave propagation normal to the layering of a layered medium.
30. T. C. T. TING 1980 *International Journal of Solids and structures* **16**, 903–911. The effects of dispersion and dissipation on wave propagation in viscoelastic layered composites.
31. G. A. BIRLIK and Y. MENGI 1987 *Journal of Sound and Vibration* **113**, 141–153. Transient wave propagation in a viscoelastic layered composite—an approximate theory.
32. L. JIANG and J. B. HADDOW 1995 *Journal of Sound and Vibration* **184**, 429–438. A finite element solution of plane wave propagation in inhomogeneous linear viscoelastic solids.
33. D. NKEMZI and W. A. GREEN 1994 *Acta Mechanica* **102**, 167–182. Transient wave propagation in a viscoelastic sandwich plate.
34. P.-C XU and A. K. MaL 1987 *Bulletin of the Seismological Society of America* **77**, 1821–1837. Calculation of the in-plane Green's function for a layered viscoelastic solid.
35. S. C. CHOU and R. GREIF 1969 *American Institute of Aeronautics and Astronautics Journal* **6**, 1067–1074. Numerical solution of stress waves in layered media.
36. D. TURHAN and Y. CALAYÍR 1991 in *Structural Dynamics*: *Recent Advances* (M. Petyt, H. G. Wolfe and C. Mei, editors) 353–362. London: Elsevier. Transient dynamic response of viscoelastic layered composites.
37. D. TURHAN, Z. CELEP and I. K. ZEIN-EDDEN 1991 *Journal of Sound and Vibration* **144**, 247–261. Transient wave propagation in layered media conducting heat.

38. Y. MENGI and A. K. TANRÍKULU 1990 *Communications in Applied Numerical Methods* **6**, 623–632. A numerical technique for two-dimensional transient wave propagation analyses.
39. A. K. TANRÍKULU, Y. MENGI and D. TURHAN 1992 *Applied Acoustics* **37**, 199–212. Propagation of out-of-plane shear waves in an elastic layer.
40. Y. MENGI and D. TURHAN 1984 *Journal of Sound and Vibration* **92**, 311–320. A higher order dynamic theory for viscoelastic plates and layered composites.
41. Y. C. FUNG 1965 *Foundations of Solid Mechanics*. Englewood Cliffs, NJ: Prentice-Hall.
42. L. E. MALVERN 1969 *Introduction to Mechanics of a Continuous Media*. New Jersey: Prentice-Hall.
43. J. L. WEGNER and J. B. HADDOW 1989 *International Journal of Engineering Sciences* **27**, 1545–1551. A note on plane wave propagation in a linear viscoelastic solid.
44. J. L. WEGNER 1993 *International Journal of Engineering Sciences* **31**, 493–508. Propagation of waves from a spherical cavity in an unbounded linear viscoelastic solid.
45. R. COURANT and D. HILBERT 1966 *Methods of Mathematical Physics*, Volume II. New York: Interscience Publishers.
46. G. B. WHITHAM 1974 *Linear and Nonlinear Waves*. New York: Wiley.
47. H. D. MCNIVEN and Y. MENGI 1971 *International Journal of Solids and Structures* **7**, 979–992. Propagation of transient, cylindrical waves in an infinite, viscoelastic body.
48. E. O. BRIGHAM 1974 *The Fast Fourier Transform*. Englewood Cliffs, NJ: Prentice-Hall.
49. J. W. COOLEY, P. A. LEWIS and P. D. WELCH 1969 *IEEE Transactions, Education* **12**, 27–34. The fast Fourier transform and its applications.
50. H. LAMB 1904 *Philosophical Transactions of the Royal Society of London*, Series **A203**, 1–42. On the propagation of tremors over the surface of an elastic solid.
51. A. S. M. ISRAEL and P. K. BANERJEE 1990 *International Journal of Solids and Structures* **26**, 851–864. Two-dimensional transient wave-propagation problems by time-domain BEM.
52. A. S. M. ISRAEL and P. K. BANERJEE 1990 *International Journal for Numerical Methods in Engineering* **29**, 1421–1440. Advanced time-domain formulation of BEM for two-dimensional transient elastodynamics.
53. B. BIRGISSON and S. L. CROUCH 1998 *International Journal for Numerical Methods in Engineering* **42**, 1045–1069. Elastodynamic boundary element method for piecewise homogeneous media.